A full-potential linear-muffin-tin-orbital molecular-dynamics study of B_7, B_{10} and B_{13} clusters

A full-potential linear-muffin-tin-orbital molecular-dynamics study of B_7, B_{10} and B_{13} clusters

Pei-lin Cao, Wei Zhao, Bao-xing Li, Bin Song and Xu-yan Zhou

Department of Physics and State Key Laboratory of Silicon Material, Zhejiang University, Hangzhou, Zhejiang 310027, China

Abstract
The structures of B_7, B_{10} and B_{13} boron clusters are studied using the full-potential linear-muffin-tin-orbital molecular-dynamics method. Seven stable structures for B_7 and fifteen for B_{10} have been obtained. C_{2h}-B_{10} is the most stable among the 15 structures, but C_{2v}-B_{10} is not stable. For B_{13}, three degenerate ground-state structures have been found. The potential surface near C_{2v}-B_7 (ground state) and D_{6h}-B_7 is very flat. As a fundamental unit in constructing bigger clusters, C_{2v}-B_7 will change its form easily. The most stable structures for B_7, B_{10} and B_{13} clusters are two-dimensional (quasi-)planar clusters, rather than the three-dimensional ones. General speaking, these clusters obey the 'Aufbau principle'.

1. Introduction

Atomic clusters represent a new phase of matter between molecules and solids, and show increasing potential for technological applications; as a result of this, their structures and energetics have been the focus of many experimental and theoretical studies in the past few years [1, 2]. The trivalent semiconductor elemental boron has a low density but a very high melting point of 2300 °C (about 1000 °C higher than that of silicon) and a high hardness similar to that of diamond. Considerable progress has been made in our understanding of the evolution of equilibrium geometries, the nature of the bonding and the electronic structure for boron. However, unlike boron crystal and boron compounds, the number of experimental and theoretical studies of boron clusters has been rather limited up to now. Hanley *et al* have measured their appearance potentials and fragmentation pattern by studying the collision-induced dissociation of ions of boron clusters containing up to 13 atoms [3]. La Placa *et al* reported the discovery of boron clusters (B_n, $n = 2$–50) formed by ablation of hexagonal boron nitride with a 532 nm laser [4]. On the theoretical side, small boron clusters were investigated by several authors using different methods [5–12]. Niu *et al* calculated the equilibrium geometries, binding energies and electronic structures of neutral and charged boron clusters containing up to six atoms [6]. Accurate calculations based on *ab initio* quantum-chemical methods were carried out for small boron clusters B_n ($n = 2$–14) to determine their electronic and geometric structures [7]. It was found that most of the final structures of the boron clusters ($n \geqslant 10$) are

composed of two fundamental units: either of hexagonal or of pentagonal pyramids; this is the so-called 'Aufbau principle'. The 'Aufbau principle' leads to four topological groups of stable boron clusters, i.e., convex, quasi-planar, tubular and spherical clusters. Applying the 'Aufbau principle', Boustani and Quandt constructed boron nanotubules of B_{24} and B_{32}, with different numbers of rings, and B_{48} using *ab initio* quantum-chemical and density functional methods to determine the relation of energy to the number of rings [10, 11]. Using *ab initio* quantum-chemical methods, Sabra and Boustani studied ground-state energies and geometrical configurations of boron and boron–hydrogen chains; they found that the ground-state energies of the boron chains were comparable to those of the boron clusters [9].

From the references cited above, it is clear that the 'Aufbau principle' is very useful as regards constructing the bigger boron clusters. For example, the decamer B_{10} results from adding three atoms to the B_7 unit. In this case the B_{10} cluster contains two similar subunits. The convex structure of the first isomer C_{2v}-B_{10} is characterized by having two top atoms, while the quasi-planar structure of the second isomer C_{2h}-B_{10} is characterized by having top and bottom atoms [7]. On adding three more B atoms, the B_{13} cluster will have three similar subunits of B_7. In order to obtain deeper insight into the structures of boron clusters and their formation from elemental units, it is worthwhile to carry out more calculations to investigate all of the possible structures for B_7, B_{10} and B_{13} clusters.

In recent years, we have studied the structures and energies of small Si_n, Ge_n and Ga_nAs_n clusters (up to $n = 60$) and the interaction between small Si clusters and NH_3, CO and H_2O using the full-potential linear-muffin-tin-orbital molecular-dynamics (FP-LMTO MD) method [13–19]. We found a series of new stable and ground-state structures. For example, our calculation found that the stable structure for the Si_{60} cluster is a distorted truncated icosahedron, with T_h symmetry. The lower symmetry and four distinct Si–Si bond lengths distinguish this structure from that with I_h symmetry and two C–C bond lengths in C_{60} [13]. Our results for Si_n and Ge_n are in good agreement with those from related experiments [20, 21]. All of our results show that the FP-LMTO MD method is an accurate way to calculate the structures of small clusters.

In the current paper, eight stable structures of B_7, fifteen stable structures of B_{10} and some of the B_{13} clusters are presented. Some consideration is given to the construction of bigger boron clusters.

2. Method

The FP-LMTO method [22–25] is a self-consistent implementation of the Kohn–Sham equations in the local-density approximation [26]. In this method, space is divided into two parts: nonoverlapping muffin-tin (MT) spheres centred at the nuclei, and the remaining interstitial region. LMTOs are augmented Hankel functions, and are augmented inside the MT spheres but not in the interstitial region [27]. In the LMTO method, one thing that we must do is to calculate the interstitial-potential matrix elements:

$$V_{ij}^I = \int_I \phi_i(x) V_I(x) \phi_j(x) \, dx \qquad (1)$$

where I is the interstitial region, V_I is the interstitial potential, i and j are abbreviations for νL and $\nu' L'$, respectively, and ϕ_i is a LMTO envelope function centred at site ν with angular momentum L. L is an abbreviation for the angular-momentum quantum numbers (l, m). In different methods, we handle V_{ij}^I in different ways. In the FP-LMTO method for clusters, Methfessel and co-workers [24, 25] used nonoverlapping MT spheres. They retained nonspherical potential terms inside the MT spheres, but expanded the interstitial potential

$V_I(x)$ in a different set of atom-centred Hankel functions. In order to obtain the interstitial-potential matrix elements, we need an accurate representation, valid in the interstitial region, of the product of two Hankel functions centred at the same site or at different sites. That is, we require an expansion of the form

$$\phi_i^* \phi_j = \sum_k C_k^{ij} \chi_k(x) \qquad (2)$$

where ϕ_i is a LMTO envelope function centred at site ν with angular momentum L. k is an abbreviation for $(\nu L \alpha)$, and the index α runs over different locations; χ_k are functions of the charge-density Hankel function set; C_k^{ij} are expansion coefficients. The interstitial-potential matrix element V_{ij}^I then reduces to a linear combination of integrals of the functions χ_k times the interstitial potential. Because the interstitial potential itself is also expanded in functions of χ_k type, the desired interstitial integral has now been expressed as a linear combination of integrals of products of pairs of Hankel functions; i.e., the three-centre integral has been reduced to a sum of two-centre integrals. Because the products are smooth functions, the coefficients in equation (2) above can be adjusted until the best fit of the values and slopes of the right-hand side to the values and slopes of the products is obtained for all spheres simultaneously by tabulation for the surfaces of the spheres. In the cluster method, the expansion is first calculated for two atoms arranged along the z-axis, and the coefficients are tabulated as functions of the interatomic distance. For a general geometry, the expansion is obtained by rotating the tabulated fit using the rotation matrices of the spherical harmonics. The tabulated fit is made by a direct numerical integration and can be made as accurate as desired [23]. The force expression for the FP-LMTO method can be obtained using the Harris energy functional [22, 23]. During the optimization of one structure, no restriction is imposed. Starting with one initial geometric configuration, we set up one time step. In each time step, the eigenvalue problem is solved exactly, and the output density is admixed with the input density in the usual way. The nuclei are then moved according to the forces using the Verlet algorithm. We then decompose the mixed density, move each partial density along with its atom, and re-overlap at the new geometry. After many iterations, the maximum of the forces is less than 0.001 au, and the total energy stays nicely constant because the system stays close to self-consistency (so the nearly zero forces agree with the energy minima). The process is stopped when the self-consistency condition is met, and a stable (or sub-stable) final calculated structure is obtained.

The details of how the molecular-dynamics simulation can be performed are described in [22, 23]. The initial structures are constructed from some consideration of symmetry. In order to have a sufficiently high probability of finding all of the local minima on the potential surface and the ground state, the number of initial structures is as large as possible based on the reasonable guesses of configurations.

3. Results and discussion

First of all, we calculated the structures for the dimer B_2 and trimer B_3. The calculated bond length of B_2 is 1.605 Å, in good agreement with the experimental value of 1.59 Å. For B_3, the final structure is triangular in shape with symmetry D_{3h}, and the resulting bond length is 1.531 Å, a little bit shorter than the result in [7]. Considering that their bond length for B_2 is 1.67 Å, 0.08 Å larger than the experimental value, we think that our calculated value for B_3 is reasonable. If the initial structure is an isosceles triangle with the angle of 28° and equal sides of 1.60 Å, our result shows that this initial structure will gradually move to D_{3h}, as found above. The average binding energies for B_2 and B_3 are 1.407 eV and 3.590 eV respectively.

3.1. B7

Seven final calculated structures are shown in figure 1, and the bond lengths, binding energies and point groups are given in table 1. These seven final structures are obtained from twenty nine initial structures. One final structure can be obtained from several different initial states. C_{2v}-B$_7$ (a in figure 1) is the most stable structure (ground state) among these seven final structures; it consists of a quasi-planar hexagon capped by a single atom 4 at a height of 0.64 Å above the plane of atoms 2, 3, 5, 7, with the atoms 1 and 6 a little bit higher (0.18 Å) than them. Our result of C_{2v}-B$_7$ is very similar to that in [7]. The average axial bond length between the apex Si atom and equatorial atoms is 1.71 Å, while that between the equatorial atoms is 1.60 Å in [7], and they are 1.69 Å and 1.59 Å respectively for our results. As for B$_2$ and B$_3$, our results are little bit shorter than those of [7]. There is in fact a final structure with higher
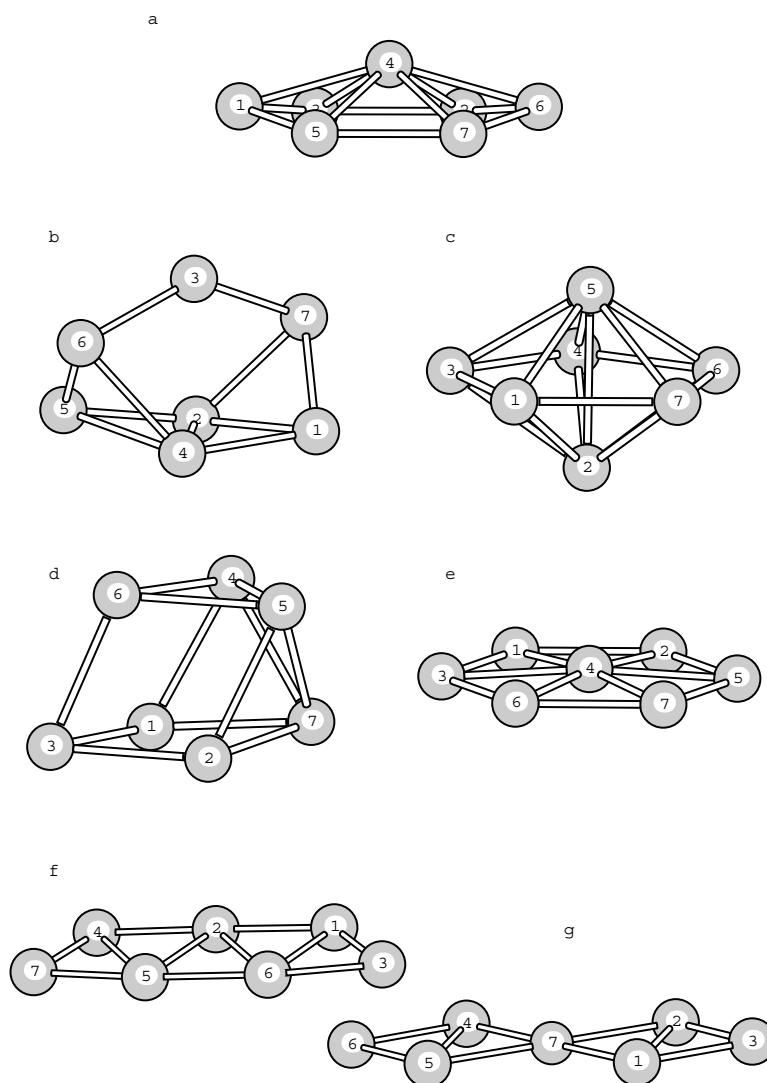

Figure 1. Geometries of the seven final stable structures of the B$_7$ cluster.

Table 1. Point groups, bond lengths (Å) and binding energies E_b and E_b/n (eV) for B_7 clusters.

Structure	Bond name	Bond length	Binding energy
a (C_{2v})	d_{41}, d_{46}	1.707	36.705 (5.244)
	d_{42}, d_{43}, d_{45}, d_{47}	1.677	
	d_{57}, d_{23}	1.629	
	d_{12}, d_{15}, d_{63}, d_{67}	1.566	
b (C_2)	d_{54}, d_{21}	1.809	35.412 (5.059)
	d_{64}, d_{72},	1.663	
	d_{36}, d_{37}	1.591	
	d_{56}, d_{17}	1.573	
	d_{41}, d_{52}	1.566	
c (quasi-D_{5h})	d_{min}: d_{45}	1.624	35.277 (5.040)
	d_{max}: d_{52}	1.804	
d (C_s)	d_{min}: d_{31}, d_{32}, d_{36}	1.652	34.786 (4.970)
	d_{max}: d_{17}, d_{64}	1.683	
e (C_{6v}, quasi-D_{6h})	d_{12}, d_{25}, d_{57}, d_{76}, d_{63}, d_{31}	1.624	36.375 (5.194)
	d_{41}, d_{42}, d_{45}, d_{47}, d_{46}, d_{43}	1.627	
f (C_{2v})	d_{min}: d_{47}, d_{13}	1.487	35.671 (5.096)
	d_{max}: d_{25}, d_{26}	1.775	
g (D_{2h})	d_{min}: d_{64}	1.517	33.710 (4.816)
	d_{max}: d_{74}	1.619	

symmetry, i.e., C_{6v}-B_7 (e in figure 1), with atom 4 only 0.10 Å higher than the hexagon plane. It is almost a D_{6h} structure (quasi-D_{6h}). The total binding energy of C_{6v}-B_7 is only 0.33 eV less than that of C_{2v}-B_7. We calculated the total energy of several structures between C_{2v}-B_7, C_{6v}-B_7 and D_{6h}-B_7. We found that all of these total energies are very close to that of C_{2v}-B_7. The maximum energy difference is only 0.34 eV in our calculations. So the potential surface is very flat in this area.

There are three three-dimensional structures in our results (b, c and d in figure 1). Their total binding energies are 1.29 eV, 1.43 eV and 1.92 eV less than that of C_{2v}-B_7. In these three three-dimensional structures, C_2-B_7 (b in figure 1) is more stable than quasi-D_{5h}-B_7 (c in figure 1) and C_i-B_7 (d in figure 1), while D_{5h}-B_7 is reported to be the optimized 3D structure in [7]. Because these three 3D structures are obtained from 15 different 3D initial structures, it is reasonable to assume that there are no other 3D structures for the B_7 cluster.

In figure 1, f and g are two chain planar structures. Their total binding energies are 1.03 eV and 2.99 eV less than that of the ground state C_{2v}-B_7. Although the binding energy of structure g is the lowest, we found that because its structure is very different from the other structures, it is a rather stable isomer. The big change in initial structure around it will not affect the final structure g.

As pointed in [12], the hexagonal pyramid is one of the basic units in the 'Aufbau principle'. According to our results mentioned above, the potential surface near C_{2v}-B_7 and quasi-D_{6h}-B_7 is very flat. When the bigger clusters are constructed from B_7 hexagonal pyramids, the form of the pyramids will change easily as a result of the interaction between them.

3.2. B_{10}

The 15 calculated final structures are shown in figure 2, and their binding energies, point groups and bond lengths for some representative structures are given in table 2. These structures are
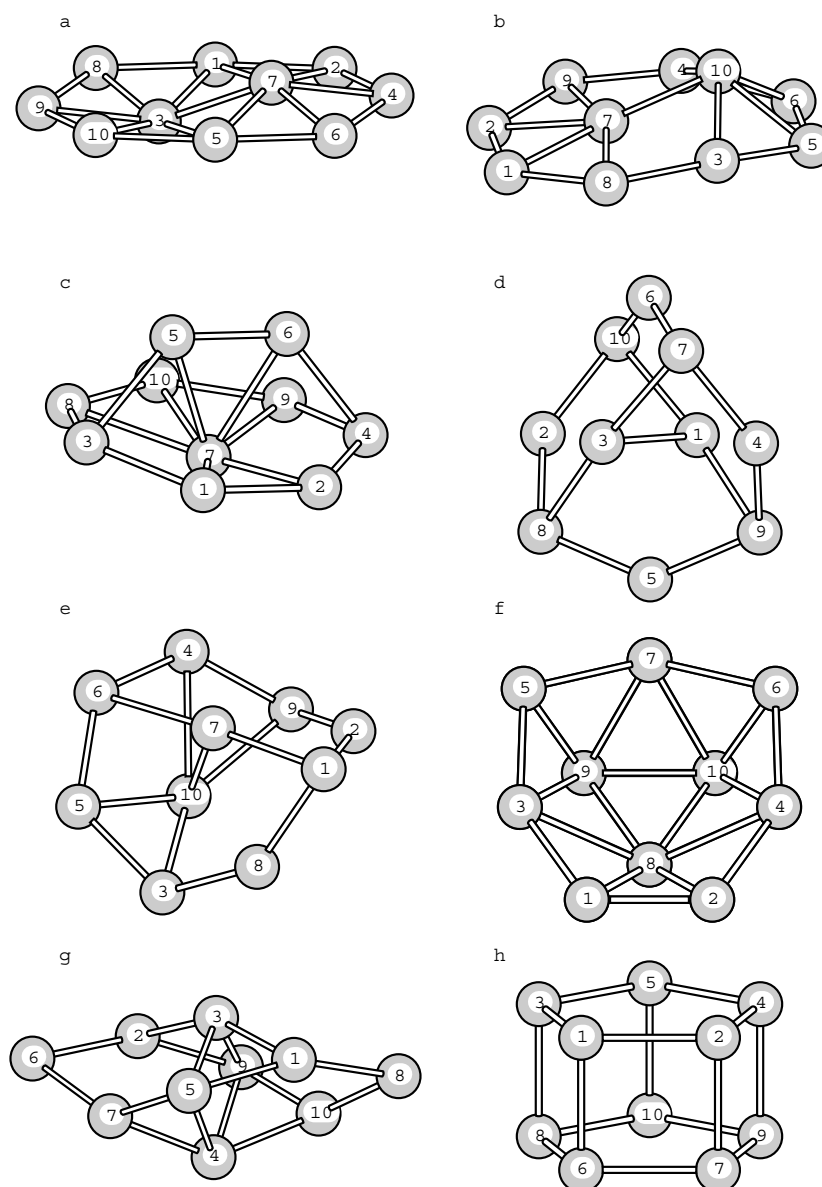
Figure 2. Geometries of the fifteen final stable structures of the B_{10} cluster.

obtained from 45 initial structures. As for B_7, one final structure can be obtained from several different initial structures. In our results, the ground-state structure is C_{2h}-B_{10}(a) (a in figure 2), a quasi-planar structure which is the same as that found in [7]. Atom 7 and atom 3 are about 0.26 Å above and below the plane of the other atoms. The average of the bond lengths between neighbouring peripheral atoms is 1.60 Å (1.60 Å); the distance between the top and bottom is 1.61 Å (1.63 Å); the averages of the bond lengths between the apices and the peripheral atoms along the short and long diagonals of the cluster are 1.75 Å (1.80 Å) and 1.64 Å (1.67 Å) respectively, where the values in parentheses are Boustani's results. In [7], it is reported that
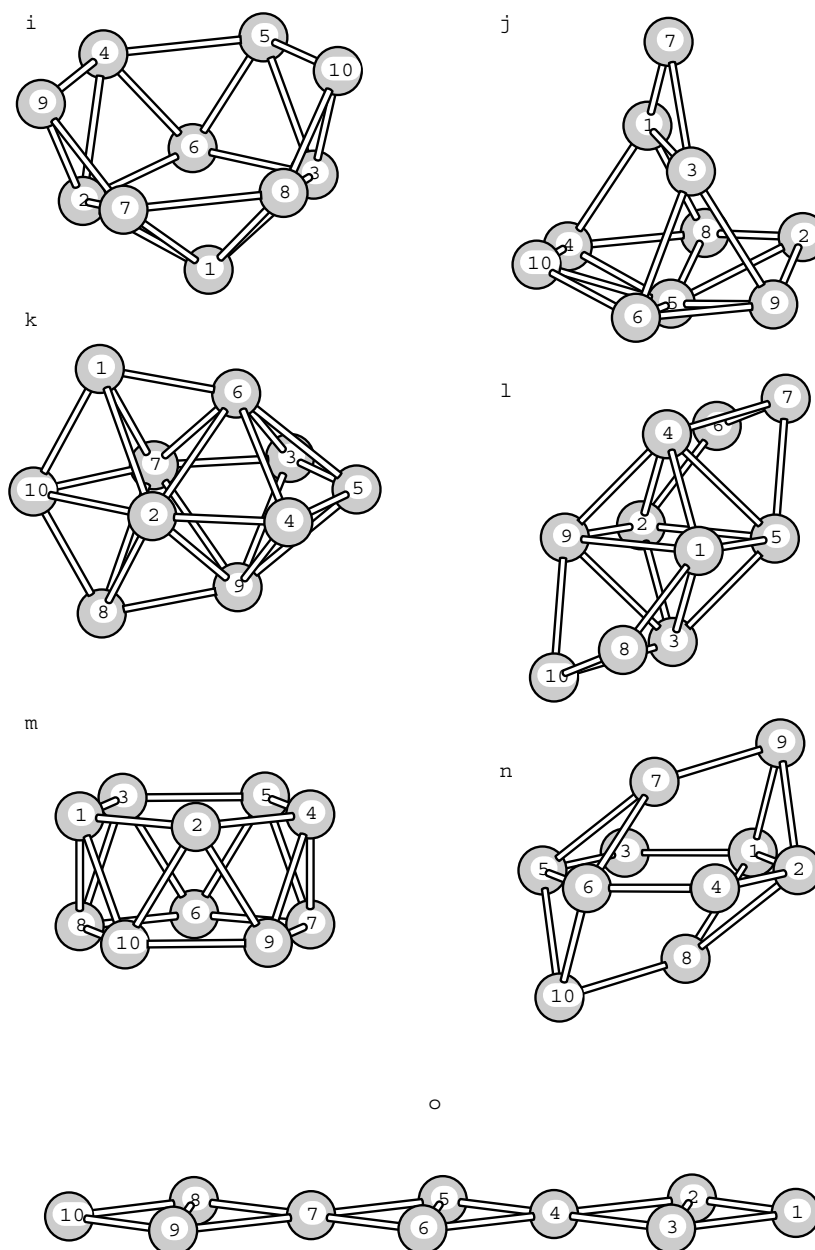
Figure 2. (Continued)

the convex structure of C$_{2v}$-B$_{10}$ has almost the same binding energy as C$_{2h}$-B$_{10}$. However, if we take C$_{2v}$-B$_{10}$ as the initial structure, our molecular-dynamics calculation shows that it will automatically change to the quasi-planar structure C$_{2h}$-B$_2$. Changing the heights of atom 3 and atom 7 in the initial structures, we get the same final structure C$_{2h}$-B$_{10}$. So we think that the convex structure of C$_{2v}$-B$_{10}$ is not stable. At the same time, as two B$_7$ pyramids construct quasi-planar B$_{10}$, the height of the apex atom will be decreased from 0.64 Å (in the B$_7$ pyramid)

Table 2. Point groups, bond lengths (Å) and binding energies E_b and E_b/n (eV) for B_{10} clusters. (For some clusters with comparatively small binding energies, just the minimum and maximum bond lengths are shown.)

Structure	Bond name	Bond length	Binding energy
a (C_{2h})	$d_{98}, d_{910}, d_{42}, d_{46}$	1.584	57.820 (5.782)
	d_{37}	1.607	
	$d_{105}, d_{65}, d_{81}, d_{21}$	1.613	
	d_{93}, d_{47}	1.625	
	$d_{72}, d_{76}, d_{38}, d_{310}$	1.647	
	$d_{57}, d_{17}, d_{53}, d_{13}$	1.745	
b (C_s)	d_{12}	1.543	57.120 (5.712)
	d_{56}	1.556	
	d_{29}, d_{18}	1.561	
	d_{83}, d_{94}	1.564	
	d_{105}, d_{106}	1.613	
	d_{35}, d_{46}	1.618	
	d_{710}	1.647	
	d_{71}, d_{72}	1.693	
	d_{103}, d_{104}	1.707	
	d_{78}, d_{79}	1.793	
c (C_s)	d_{56}	1.538	56.717 (5.672)
	d_{38}, d_{49}	1.557	
	d_{12}	1.560	
	d_{810}, d_{910}	1.571	
	d_{31}, d_{42}	1.590	
	d_{53}, d_{64}	1.682	
	d_{710}	1.720	
	d_{71}, d_{72}	1.735	
	d_{57}, d_{67}	1.801	
	d_{78}, d_{79}	1.836	

to 0.26 Å in C_{2h}-B_{10}. B_{10}(b) (b in figure 2) is a new structure never reported before; its binding energy is only little bit smaller than that of the ground state B_{10}(a). There is only one apex atom (atom 10 in figure 2), and the other atoms are almost on the same plane. The height of the apex atom is about 0.52 Å.

Comparing with B_7, the number of three-dimensional structures (B_{10}(c) to B_{10}(n) in figure 2) is greatly increased. Our 12 final 3D structures are obtained from 39 different initial structures. We think that it would be hard to obtain more new 3D structures, especially clusters with comparatively large binding energies. The binding energy of B_{10}(c) is the largest among all of these 3D structures, but it is still 1.10 eV smaller than that of the ground state C_{2h}-B_{10}. The binding energy of B_{10}(n) is the smallest among the 3D structures, 4.37 eV smaller than that of B_{10}(a). In the B_7 cluster, there is a planar structure of quasi-C_{6h} symmetry (B_7(e) in figure 1), but in B_{10} there is no similar planar structure. If we take this structure as the initial state (height = 0 for apex atom 3 and atom 7 as mentioned above), it will automatically change to B_{10}(a).

There is a chain structure in B_{10} clusters (B_{10}(o) in figure 2). Its binding energy per atom is 5.0185 eV, 0.764 eV less than that of the ground state B_{10}(a). Although the binding energy of B_{10}(o) is the smallest among the B_{10} clusters, like B_7(g) it is a rather stable structure.

Table 2. (Continued.)

Structure	Bond name	Bond length	Binding energy
d (C$_{2v}$, quasi-D$_{2d}$)	$d_{67}, d_{610}, d_{58}, d_{59}$ and $d_{47}, d_{49}, d_{210}, d_{28}$	1.542	55.931 (5.593)
	$d_{19}, d_{110}, d_{37}, d_{38}$	1.703	
	d_{31}	1.843	
e (C$_1$)	d_{min}: $d_{12}, d_{18}, d_{64}, d_{65}$	1.537	55.886 (5.589)
	d_{max}: d_{710}	1.864	
f (C$_s$)	d_{min}: d_{12}	1.526	55.589 (5.559)
	d_{max}: d_{38}, d_{48}	1.789	
g (C$_2$)	d_{min}: d_{29}, d_{15}	1.556	54.773 (5.477)
	d_{max}: d_{39}, d_{35}	1.743	
h (D$_{5h}$)	d_{12}	1.587	54.619 (5.462)
	d_{16}	1.588	
i (C$_s$)	d_{min}: d_{92}, d_{103}	1.574	54.614 (5.461)
	d_{max}: d_{45}	1.792	
j (C$_{2v}$)	d_{min}: d_{71}, d_{73}	1.542	54.462 (5.446)
	d_{max}: d_{13}	1.819	
k (C$_{2v}$)	d_{min}: $d_{89}, d_{16}, d_{37}, d_{42}$	1.545	54.458 (5.446)
	d_{max}: $d_{94}, d_{93}, d_{64}, d_{63}$ and $d_{28}, d_{21}, d_{78}, d_{71}$	1.890	
l (C$_i$)	d_{min}: d_{810}, d_{67}	1.535	54.431 (5.443)
	d_{max}: $d_{19}, d_{13}, d_{24}, d_{25}$	1.869	
m (D$_{5d}$)	d_{18}, d_{110}	1.586	53.841 (5.385)
	d_{109}, d_{12}	1.588	
n (C$_i$)	d_{min}: $d_{53}, d_{13}, d_{46}, d_{42}$	1.568	53.447 (5.345)
	d_{max}: d_{56}, d_{12}	1.723	
o (D$_{2h}$)	d_{min}: $d_{910}, d_{810}, d_{12}, d_{13}$	1.511	50.185 (5.019)
	d_{max}: $d_{87}, d_{97}, d_{42}, d_{43}$	1.640	

3.3. B$_{13}$

In B$_7$ and B$_{10}$ clusters, the binding energy of the two-dimensional structures is higher than that of the 3D structures. The two-dimensional structures are more stable. For B$_{13}$, we only studied the two-dimensional structures at this stage.

Five calculated final structures are shown in figure 3, and their binding energies, point groups and bond lengths are given in table 3.

In these five final structures, B$_{13}$(a), (b) and (d) are almost degenerate. The total binding energy of (d) is 0.05 eV greater than that of (a) and 0.09 eV greater than that of (b). The atoms in (a) and (d) are almost on the same plane: in (a), atoms 6 (and 8) and 7 are only 0.12 Å and 0.09 Å above the other atoms. In (d), the biggest height difference is less than 0.1 Å. The
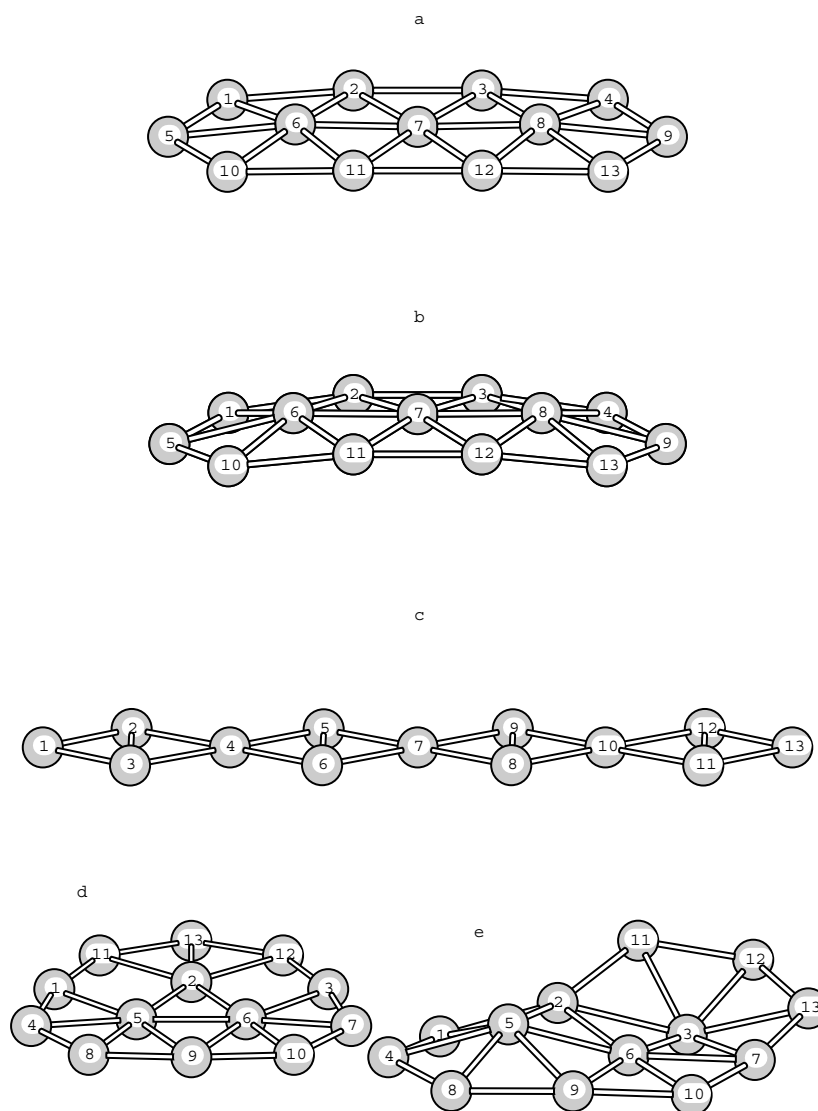
Figure 3. Geometries of the five final stable two-dimensional (quasi-) planar clusters of B_{13}.

structure of B_{13}(b) is very similar to that of (a), except that its atoms are not on the plane but on the surface of a arch, producing a convex structure. For B_{13}(e), compared with (a) and (d), three more atoms are added on the corner of B_{10}(a), whose total binding energy is 0.91 eV less than that of B_{13}(a), and the cluster has lost all symmetry. In B_{13}(e), atoms 1 and 3 have moved down by about 0.30 Å and 0.37 Å, while atoms 5, 11 and 12 have moved up by about 0.39, 0.43 and 0.16 Å respectively; the other atoms are almost on the same plane. General speaking, this cluster is still constructed of three hexagonal pyramids, although they are deformed. However, the ground state B_{13}(d) is a new structure, only containing two hexagonal pyramids (in fact, two quasi-D_{6h} structures).

Our final structure, B_{13}(b), is similar to the convex structure C_{2v}-B_{13} of Boustani, but our structure is flatter. The average of the bond lengths between the peripheral atoms is 1.60 Å

Table 3. Point groups, bond lengths (Å) and binding energies E_b and E_b/n (eV) for B_{13} clusters.

Structure	Bond name	Bond length	Binding energy
a (C_{2v})	d_{67}, d_{78}	1.554	77.171 (5.936)
	d_{51}, d_{510}, d_{94}, d_{913}	1.593	
	d_{12}, d_{1011}, d_{34}, d_{1213}	1.609	
	d_{56}, d_{89}	1.621	
	d_{23}, d_{1112}	1.631	
	d_{16}, d_{106}, d_{48}, d_{138}	1.656	
	d_{26}, d_{116}, d_{38}, d_{128}	1.732	
	d_{27}, d_{37}, d_{117}, d_{127}	1.765	
b (C_{2v})	d_{67}	1.575	77.125 (5.933)
	d_{51}	1.588	
	d_{12}	1.607	
	d_{56}	1.626	
	d_{23}	1.630	
	d_{16}	1.662	
	d_{26}	1.741	
	d_{27}	1.765	
c (D_{2h})	d_{min}: d_{12}	1.513	66.253 (5.096)
	d_{max}: d_{24}	1.650	
d (C_{2v})	d_{107}	1.529	77.218 (5.940)
	d_{1113}	1.532	
	d_{123}	1.547	
	d_{41}	1.575	
	d_{89}	1.588	
	d_{45}	1.645	
	d_{85}	1.669	
	d_{56}	1.686	
	d_{213}	1.690	
	d_{52}	1.777	
	d_{15}	1.806	
	d_{59}	1.811	
e (C_1)	d_{min}: d_{1213}	1.541	76.292 (5.610)
	d_{max}: d_{23}	1.773	

(1.60 Å), that between the central atom and the four peripheral atoms is 1.77 Å (1.83 Å) and each of the other two apex atoms bonds to the three neighbouring atoms at a distance of 1.65 Å (1.70 Å), where the values in parentheses are Boustani's results.

There is a chain structure of $B_{13}(c)$ similar to the structure of $B_{10}(o)$ in figure 2. Its binding energy per atom is 5.0964 eV, 0.890 eV less than that of $B_{13}(d)$.

4. Conclusions

For B_7, the ground-state structure is C_{2v}-$B_7(a)$. There are three 3D structures. Their binding energies are 1.29 eV, 1.43 eV and 1.92 eV higher than that of $B_7(a)$. The potential surface near C_{2v}-$B_7(a)$ and quasi-D_{6h}-$B_7(e)$ is very flat.

For B_{10}, the ground state is C_{2h}-$B_{10}(a)$, but the convex structure of C_{2v}-B_{10} is not stable in our MD calculation: it will automatically transform to C_{2h}-$B_{10}(a)$. There is a new quasi-planar structure, $B_{10}(b)$; it is only 0.70 eV higher than that of C_{2h}-B_{10}. There are twelve 3D clusters in B_{10}. Their total binding energies are 1.10 eV to 4.37 eV less than that of C_{2h}-B_{10}.

C_{2v}-B_{13}(d) is the ground-state structure of the B_{13} cluster, but B_{13}(a) and B_{13}(b) are almost degenerate with it.

Comparing the ground-state structures of B_7, B_{10} and B_{13}, the B_{13} cluster is almost planar, much flatter than B_7. The bigger the cluster, the flatter it will be. In other words, the structure will get nearer to the ideal sp^2 with increasing number of B atoms in the cluster.

It is suggested that the boron clusters grow according to the 'Aufbau principle'. Starting from the basic unit, the hexagonal pyramid B_7, and adding atoms sequentially, one can form new hexagonal pyramids to obtain either quasi-planar or convex structures [7]. B_{10} has two hexagonal pyramids and B_{13} has three. In our final structures, B_{10} is a quasi-planar structure, but the convex structure is not stable. For B_{13}, three degenerate ground states cannot be distinguished clearly as quasi-planar or convex structures, and B_{13}(d) does not consist of three hexagonal pyramids. It seems that although the 'Aufbau principle' is very useful in describing the growth of boron clusters, the process is more complicated than that predicted by the principle.

Acknowledgment

References

[1] Bernstein E R (ed) 1989 *Atomic and Molecular Clusters (Studies in Physical and Theoretical Chemistry vol 68)* (Amsterdam: Elsevier)
[2] Jena P, Rao B K and Khanna S N (ed) 1990 *Physics and Chemistry of Small Clusters (NATO ASI Series vol 158)* (Dordrecht: Kluwer)
[3] Hanley L, Whitten J L and Anderson S L 1988 *J. Phys. Chem.* **92** 5803
[4] La Placa S J, Roland P A and Wynne J J 1992 *Chem. Phys. Lett.* **190** 163
[5] Kato H and Yamashita K 1992 *Chem. Phys. Lett.* **190** 361
[6] Niu J, Rao B K and Jena P 1997 *J. Chem. Phys.* **107** 132
[7] Boustani I 1997 *Phys. Rev.* B **55** 16 426
[8] Ricca A and Bauschlicher C W Jr 1996 *Chem. Phys.* **208** 233
[9] Sabra M K and Boustani I 1998 *Europhys. Lett.* **42** 611
[10] Boustani I and Quandt A 1997 *Europhys. Lett.* **39** 527
[11] Boustani I and Quandt A 1998 *Comput. Mater. Sci.* **11** 132
[12] Boustani I 1995 *Chem. Phys. Lett.* **240** 135
[13] Li Bao-xing, Cao P L and Que D L 2000 *Phys. Rev.* B **61** 1685
[14] Li B X, Cao P L and Jiang M 2000 *Phys. Status Solidi* b **218** 399
[15] Li B X and Cao P L 2000 *Phys. Status Solidi* b **219** 253
[16] Li B X, Qiu M and Cao P L 1999 *Phys. Lett.* A **256** 386
[17] Li B X, Jiang M and Cao P L 1999 *J. Phys.: Condens. Matter* **11** 8517
[18] Qiu M, Jiang M, Zhao Y J and Cao P L 1999 *J. Chem. Phys.* **110** 10 738
[19] Qiu M, Zhou X Y, Jiang M and Cao P L 1998 *Phys. Lett.* A **245** 430
[20] Jarrold M F, Ijiri Y and Ray U 1991 *J. Chem. Phys.* **94** 3607
[21] Creasy W R, O'Keefe A, and McDonald J R 1987 *J. Phys. Chem.* **91** 2848
[22] Methfessel M and Schilfgaarde M V 1993 *Int. J. Mod. Phys.* B **7** 262
[23] Methfessel M and Schilfgaarde M V 1993 *Phys. Rev.* B **48** 4937
[24] Methfessel M 1988 *Phys. Rev.* B **38** 1537
[25] Methfessel M, Rodriguez C O and Anderson O K 1989 *Phys. Rev.* B **40** 2009
[26] Kohn W and Sham L J 1965 *Phys. Rev.* A **140** 1133
[27] Anderson O K 1975 *Phys. Rev.* B **12** 3060
[28] Huber K P and Herzberg G 1979 *Molecular Spectra and Molecular Structure Constants of Diatomic Molecules vol 4* (New York: Van Nostrand-Reinhold)